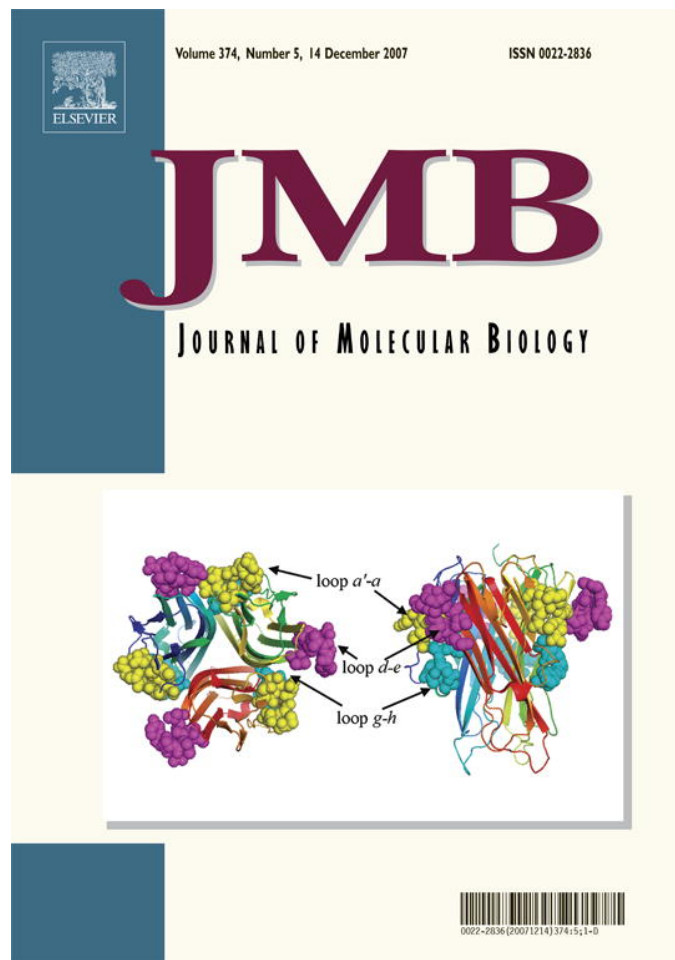


Provided for non-commercial research and education use.
Not for reproduction, distribution or commercial use.



This article was published in an Elsevier journal. The attached copy is furnished to the author for non-commercial research and education use, including for instruction at the author's institution, sharing with colleagues and providing to institution administration.

Other uses, including reproduction and distribution, or selling or licensing copies, or posting to personal, institutional or third party websites are prohibited.

In most cases authors are permitted to post their version of the article (e.g. in Word or Tex form) to their personal website or institutional repository. Authors requiring further information regarding Elsevier's archiving and manuscript policies are encouraged to visit:

<http://www.elsevier.com/copyright>

JMBAvailable online at www.sciencedirect.com

ScienceDirect


***Haloferax volcanii* AgIB and AgID are Involved in N-glycosylation of the S-layer Glycoprotein and Proper Assembly of the Surface Layer**

**Mehtap Abu-Qarn¹, Sophie Yurist-Doutsch¹, Assunta Giordano²
 Andrej Trauner³, Howard R. Morris^{3,4}, Paul Hitchen³
 Ohad Medalia^{1,5}, Anne Dell³ and Jerry Eichler^{1*}**

¹*Department of Life Sciences
 Ben Gurion University
 Beersheva 84105, Israel*

²*Istituto di Chimica
 Biomolecolare, Consiglio
 Nazionale delle Ricerche
 Pozzuoli (NA) 80078, Italy*

³*Division of Molecular
 Biosciences, Faculty of Life
 Sciences, Imperial College
 London SW7 2AZ, UK*

⁴*M-SCAN Ltd, Wokingham
 Berkshire, RG41 2TZ, UK*

⁵*National Institute for
 Biotechnology in the Negev
 Ben Gurion University
 Beersheva 84105, Israel*

Received 26 August 2007;
 received in revised form
 7 October 2007;
 accepted 16 October 2007
 Available online
 22 October 2007

In this study, the effects of deleting two genes previously implicated in *Haloferax volcanii* N-glycosylation on the assembly and attachment of a novel Asn-linked pentasaccharide decorating the *H. volcanii* S-layer glycoprotein were considered. Mass spectrometry revealed the pentasaccharide to comprise two hexoses, two hexuronic acids and an additional 190 Da saccharide. The absence of AgID prevented addition of the final hexose to the pentasaccharide, while cells lacking AgIB were unable to N-glycosylate the S-layer glycoprotein. In AgID-lacking cells, the S-layer glycoprotein-based surface layer presented both an architecture and protease susceptibility different from the background strain. By contrast, the absence of AgIB resulted in enhanced release of the S-layer glycoprotein. *H. volcanii* cells lacking these N-glycosylation genes, moreover, grew significantly less well at elevated salt levels than did cells of the background strain. Thus, these results offer experimental evidence showing that N-glycosylation endows *H. volcanii* with an ability to maintain an intact and stable cell envelope in hypersaline surroundings, ensuring survival in this extreme environment.

© 2007 Elsevier Ltd. All rights reserved.

Edited by J. Karn

Keywords: Archaea; glycosyltransferase; N-glycosylation; oligosaccharyltransferase; surface-layer glycoprotein

*Corresponding author. E-mail address: jeichler@bgu.ac.il.
 URL: <http://www.bgu.ac.il/life/Faculty/Eichler/index.htm>.

Present address: J. Eichler, Department of Life Sciences, Ben Gurion University, PO Box 653, Beersheva 84105, Israel.

Abbreviations used: ER, endoplasmic reticulum; OST, oligosaccharyltransferase; MS, mass spectrometry; MALDI TOF, Matrix-assisted laser desorption/ionization time of flight; EM, electron microscopy.

Introduction

N-linked protein glycosylation is one of the most common and versatile post-translational modifications and is experienced by proteins in all three domains of life.^{1–4} The process is best understood in Eukarya, where N-glycosylation begins with assembly of a dolichol pyrophosphate-linked oligosaccharide on the cytoplasmic face of the endoplasmic reticulum (ER).^{1,4–7} This lipid-linked oligosaccharide is then reoriented to face the ER lumen, where additional sugar subunits are added. The completed

oligosaccharide is then transferred, *en bloc*, to selected Asn residues of secretory pathway proteins by the oligosaccharyltransferase (OST) complex.^{8,9} Immediately following attachment of the oligosaccharide to a target protein, a series of glycan remodeling steps that begin in the ER and continue in the Golgi is initiated. The importance of N-glycosylation to Eukarya is reflected by the various roles this post-translational modification plays in protein folding, oligomerization and quality control.⁷

While it has long been known that eukaryal proteins experience N-glycosylation, it was only recently shown that N-glycosylation also occurs in Bacteria.³ The bacterial N-glycosylation pathway has been best described in the food-borne pathogen, *Campylobacter jejuni*, shown to contain an N-glycosylation machinery encoded by the 12 genes of the *pgl* locus.^{10,11} N-glycosylation in *C. jejuni* relies on a simpler pathway than does the parallel eukaryal process, with a heptameric polysaccharide being assembled on a cytoplasmically oriented undecaprenol lipid carrier lying in the plasma membrane.^{12,13} The oligosaccharide-loaded lipid is then “flipped” to face the cell exterior and the glycan moiety is transferred to select Asn residues of target proteins by PglB.^{14,15} In *C. jejuni*, at least 30 proteins have been shown to contain N-linked glycans, where they are implicated in pathogenicity *via* mediation of host–cell adherence, invasion and colonization.^{16–18}

In contrast to the relatively well-defined pathways of N-glycosylation in Eukarya and Bacteria, only little is known of the steps involved in archaeal N-glycosylation, despite the fact that the first example of a prokaryal glycoprotein, the *Halobacterium salinarum* surface (S)-layer glycoprotein, came from an archaeal source.^{19,20} Indeed, N-glycosylated proteins are far more abundant in Archaea than in Bacteria^{21,22} and include S-layer glycoproteins and flagellins, as well as various membrane and secreted proteins.² Thus, while N-glycosylation is relatively common in Archaea, the molecular mechanism of this processing event has only recently begun to attract attention. Chaban *et al.*²³ reported on the effects of insertional inactivation of two genes involved in the biogenesis

and attachment of a trisaccharide found on flagellins and the S-layer glycoprotein of the methanogen *Methanococcus voltae*. At the same time, work in the Eichler laboratory showed that deletion of *Haloferax volcanii* genes encoding homologues to the eukaryal OST catalytic subunit, Stt3, and a phosphodolichol glucosyltransferase, Alg5, affected S-layer glycoprotein glycosylation, as demonstrated *via* glycostaining and changes in apparent molecular weight.²⁴

Here, the roles played by the *H. volcanii* homologues of Stt3 and Alg5, now renamed AglB and AglD, respectively, according to the nomenclature of Chaban *et al.*,²³ in the N-glycosylation of the *H. volcanii* S-layer glycoprotein were investigated. In addition, the importance of correct N-glycosylation of the S-layer glycoprotein for *H. volcanii* physiology and survival was explored.

Results

H. volcanii AglD is a homologue of eukaryal Alg5

Earlier work²⁴ reported that *H. volcanii* encodes homologues of eukaryal and bacterial proteins involved in N-glycosylation. Of these, one of the two *H. volcanii* homologues of eukaryal Alg5 detected, termed Alg5-A, was implicated in the glycosylation of a reporter glycoprotein, the S-layer glycoprotein. Now, employing the terminology for archaeal genes involved in N-glycosylation (the archaeal glycosylation genes) proposed by Chaban *et al.*,²³ *H. volcanii* *alg5-A* has been renamed *aglD*. Conserved domain prediction²⁵ indicates *H. volcanii* AglD to contain a glycosyltransferase 2 family domain (Pfam 00535, COG1216) as well as a second region predicted to belong to the Pfam03706 group, corresponding to an uncharacterized protein family (UPF0104) that includes members annotated as dolichol-P-glucose synthases that also contain a Pfam 00535 domain.

BLAST-based searches of several genomes revealed the presence of AglD homologues in

Figure 1. Archaeal and eukaryal homologues of *H. volcanii* AglD. (a) Phylogenetic tree of *H. volcanii* AglD and its archaeal and eukaryal homologues, generated by ClustalX (version 1.83) from a multiple sequence alignment created by T-coffee and drawn by TreeView (version 1.6.6; taxonomy.zoology.gla.ac.uk/rod/treeview.html). The bootstrap values shown correspond to confidence levels obtained upon 1000 trial repeats. The archaeal sequences shown come from *Aeropyrum pernix* (NP_147774.1; Aper), *Archaeoglobus fulgidus* (NP_069415.1; Aful), *Haloarcula marismortui* (YP_136461.1; Hmar), *Halobacterium* sp. NRC-1 (NP_279416.1; HNRC), *Haloferax volcanii* (Hvol), *Haloquadratum walsbyi* (YP_657261.1; Hwal), *Metallosphaera sedula* (ZP_01601347.1; Msed), *Methanopyrus kandleri* (NP_614163.1; Mkan), *Methanosarcina acetivorans* (NP_618739.1; Mace), *Methanosarcina barkeri* (YP_304067.1; Mbar), *Methanospirillum hungatei* (YP_503949.1; Mhun), *Natronomonas pharaonis* (YP_326773.1; Npha), *Picrophilus torridus* (YP_024256.1; Ptor), *Pyrococcus abyssi* (NP_127133.1; Paby), *Sulfolobus solfataricus* (NP_342803.1; Ssol), *Thermococcus kodakarensis* (YP_182777.1; Tkod) and *Thermoplasma volcanium* (NP_111403.1; Tvol), while the eukaryal sequences shown come from *Aedes aegypti* (ABF18373.1; Aep), *Candida albicans* (XP_715818.1; Calb), *Dictyostelium discoideum* (AAQ98885.1; Ddis), *Gallus gallus* (XP_417093.2; Ggal), *Homo sapiens* (AAG09682.1; Hsap), *Mus musculus* (NP_079718.1; Mmus), *Saccharomyces cerevisiae* (NP_015097.1; Scer) and *Xenopus laevis* (AAH44127.1; Xlae) (b) The deduced amino acid sequence of *H. volcanii* AglD was compared with the sequences of the *Saccharomyces cerevisiae* ALG5 protein (NP_015097.1; Scer) and *Homo sapiens* dolichyl-phosphate β -glucosyltransferase (AAG09682.1; Hsap). The nucleotide sequence of *H. volcanii* *aglD* has been deposited in the EMBL nucleotide sequence database (accession number AM698042). The bold, underlined residues correspond to predicted transmembrane domains.

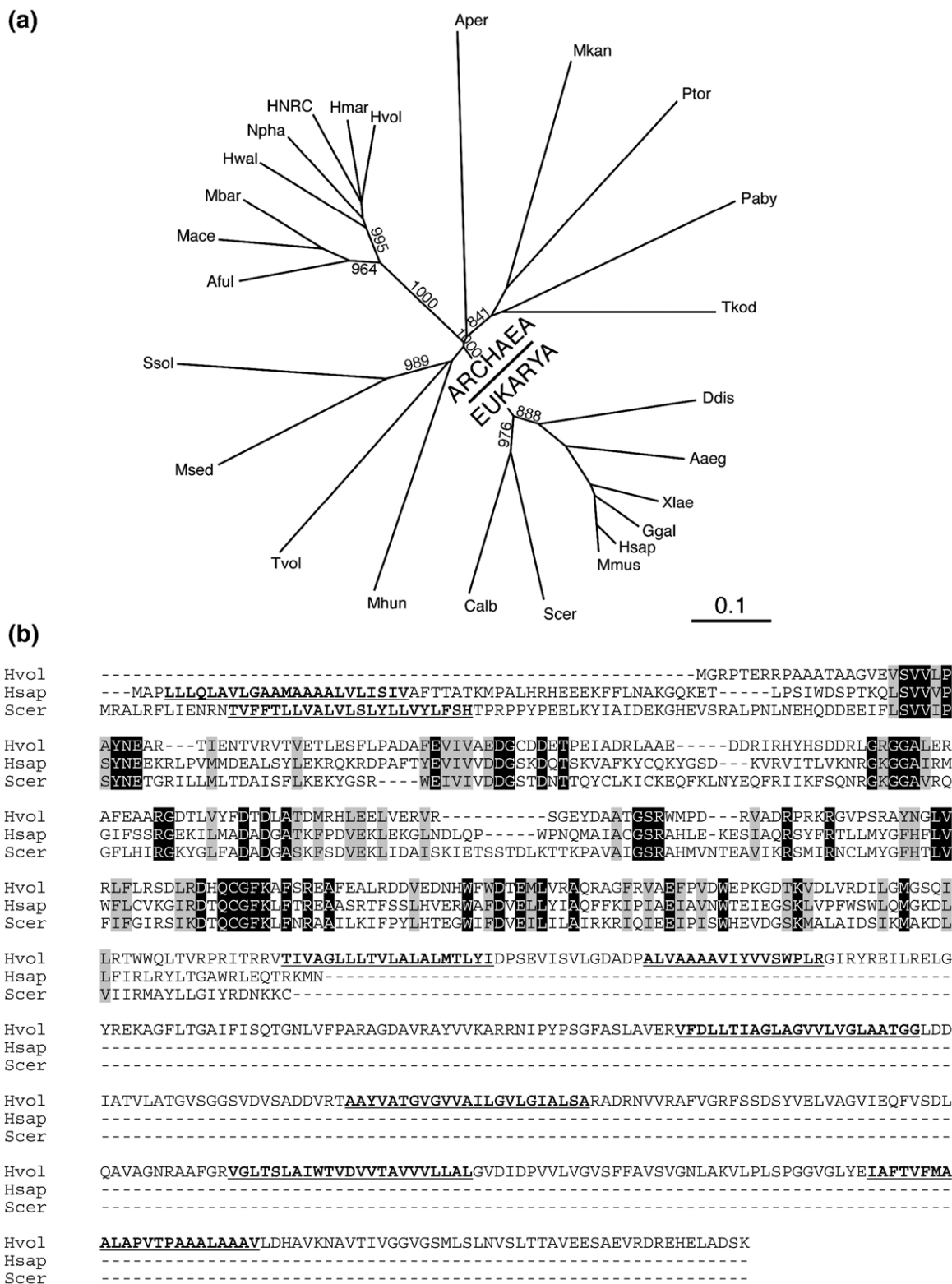


Figure 1 (legend on previous page)

other archaeal species (Figure 1(a)), although none have been characterized functionally. Alignment† of the N-terminal halves of these AgID-like sequences reveals several highly conserved motifs that may

† align.genome.jp; www.ch.embnet.org/software/TCoffee.html

participate in the proposed glycosyltransferase activity of the proteins (data not shown). While *H. volcanii* AgID was originally identified through its similarity to *Saccharomyces cerevisiae* ALG5 and its homologues in other Eukarya, phylogenetic analysis reveals that archaeal AlgD proteins form a clade distinct from their eukaryal homologues (Figure

1(a)). Indeed, as presented in Figure 1(b), *H. volcanii* AglD can be clearly distinguished from *S. cerevisiae* ALG5 or its human homologue in terms of membrane topology. The topology prediction tools TMHMM‡ and HMMTOP§ describe *H. volcanii* AglD as an integral membrane protein presenting a large internally oriented N-terminal half and a C-terminal half comprising six membrane-spanning domains including three short externally oriented loops. By contrast, the homologous human and yeast proteins are thought to contain a single transmembrane domain, located almost immediately downstream of the N terminus.

AgID participates in *H. volcanii* S-layer glycoprotein N-glycosylation

To better describe the contribution of AglD to *H. volcanii* protein glycosylation, a detailed examination of both the N-glycosylation profile of the S-layer glycoprotein, a well-described reporter of this post-translational modification,^{26–29} and the contribution of AglD to this processing event, was undertaken. Initially, horseradish peroxidase (HRP)-conjugated concanavalin A (ConA) was employed in a lectin overlay protocol to probe the S-layer glycoprotein in background and *aglD*-deleted cells²⁹ as well as in cells lacking *alg5-B*, an *aglD* homologue (Figure 2(a)).²⁴ While the lectin recognized the S-layer glycoprotein in all three cell types, the labeled band from the *aglD*-deleted strain migrating slightly faster on SDS-PAGE gels than did the protein from the background or Alg5B-lacking strains, in agreement with earlier observations.²⁴ In a second experiment, the background and *aglD*-lacking strains were grown in minimal medium and incubated with [¹⁴C] glucose, -galactose or -mannose. As in earlier analyses of the *H. volcanii* glycoprotein pool²⁸ and of the S-layer glycoprotein in particular,^{27,30} incubation with the radiolabeled sugars led to labeling of the S-layer glycoprotein, albeit to differing degrees in each strain (Figure 2(b)). Densitometric quantification of the relative amounts of radioactive glucose, galactose and mannose incorporated into comparable amounts (as deemed by Coomassie staining and densitometry) of the S-layer glycoprotein from triplicate samples of the background strain yielded a 1.0:0.7:0.1 ratio, in agreement with earlier reports of the relative content of the three saccharides in the *H. volcanii* glycoprotein pool.²⁸ When the same strain lacking *aglD* was grown under similar conditions, all three radiolabeled sugars were once again incorporated into the S-layer glycoprotein, as revealed by SDS-PAGE and fluorography. In these cells, however, glucose, galactose and mannose were found in a 1.0:0.1:0.1 ratio, averaged over three experiments. Thus, the efficiencies of [¹⁴C]glucose, -galactose and -mannose-based modification of the S-layer glycoprotein in the background and *aglD*-deleted strains are clearly distinct.

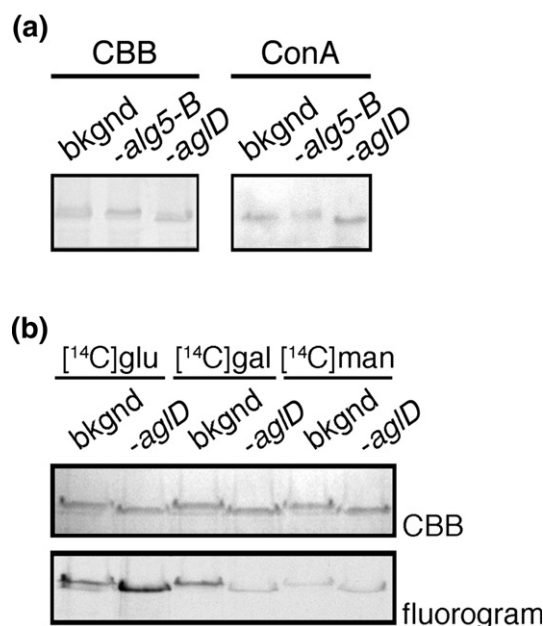


Figure 2. Glycosylation of the *H. volcanii* S-layer glycoprotein differs in the presence or absence of *aglD*. (a) The protein contents of *H. volcanii* WR536 background cells (bkgnd) as well as proteins of the same strain lacking either Alg5-B (*-alg5-B*) or AglD (*-aglD*) were separated by SDS-7.5% (w/v) PAGE and subjected to Coomassie staining (left panel) or overlay with HRP-conjugated ConA (right panel). (b) *H. volcanii* WR536 cells (bkgnd) or the same strain lacking AglD (*-aglD*) were grown in the presence of [¹⁴C]glucose, -galactose or -mannose and subjected to Coomassie staining (upper panel) or fluorography (lower panel). In both (a) and (b), only the S-layer glycoprotein is shown.

AgID is involved in the addition of the final hexose subunit to a pentasaccharide decorating the *H. volcanii* S-layer glycoprotein

Efforts next focused on mass spectrometric (MS) characterization of the glycosylation pattern of the S-layer glycoprotein reporter in AglD-lacking cells. SDS-PAGE gel pieces from the background and mutant strains containing the S-layer glycoprotein were subjected to in-gel tryptic digestion and the obtained peptides were separated by liquid chromatography. MS/MS was then employed to reveal peptide sequences. As such, six peptide sequences were obtained, including two containing potential N-glycosylation sites. Of these, the N-terminal ¹ERGNLDADESEFNK¹⁴ peptide (1581 *m/z*) was of particular interest, given that it contains a N-glycosylation site previously reported as being modified.²⁶ The glycan content of the Asn13-containing S-layer glycoprotein-derived peptide from the background strain was determined by Matrix-assisted laser desorption/ionization time of flight (MALDI TOF) mass mapping of the nanoLC-purified tryptic digest, complemented by MS/MS analyses using MALDI TOF/TOF and electrospray Q-TOF instrumentation. The MALDI spectrum (Figure 3(a)) revealed the presence of a pentasaccharide moiety

‡ www.cbs.dtu.dk/services/TMHMM-2.0

§ www.enzim.hu/hmmtop

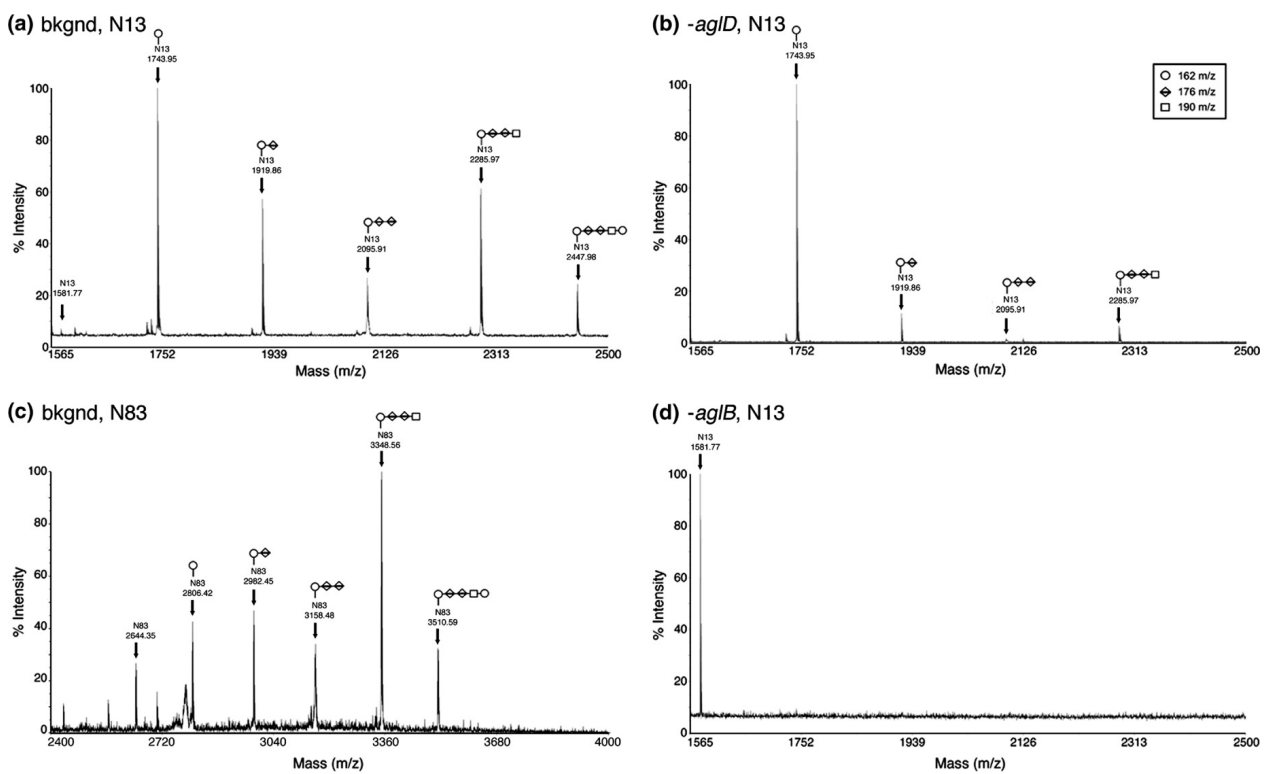


Figure 3. MALDI TOF analysis of *H. volcanii* S-layer glycoprotein-derived glycopeptides. Shown are MALDI spectra obtained from the Asn13-containing tryptic glycopeptides from (a) the background and (b) the *agID* deletion strains. (c) MALDI spectrum of the Asn83-containing tryptic/Glu-C glycopeptide from the background strain. (d) MALDI spectrum of the unmodified Asn13-containing peptide from the *agIB* deletion strain. The nature of the glycopeptide-associated sugar residues is shown in the inset of (b). Tryptic peptides were separated by offline nanoLC prior to analysis.

(m/z 2447), as well as precursors bearing mono- (m/z 1743), di- (m/z 1919), tri- (m/z 2095) and tetrasaccharides (m/z 2285). These data suggest that the Asn13-linked pentasaccharide is comprised of a hexose (162 Da), followed by two 176 Da residues, one 190 Da residue and an additional hexose residue at the end of the chain. MS/MS experiments on each glycoform gave data consistent with this conclusion (results not shown). To assess the nature of the two 176 Da residues, the tryptic digest was methyl esterified in 2 M HCl/MeOH, purified by nanoLC and analyzed by MALDI TOF. Under these conditions, all carboxylic acid moieties are converted to their methyl esters, resulting in a mass shift of 14 Da for each carboxylic acid. As predicted, the peptide modified by a single hexose residue (m/z 1743; Figure 3(a)) shifted to m/z 1813 (data not shown), consistent with the five carboxylic acids known to be present in the peptide (two Glu, two Asp and one C terminus). By contrast, the peptide modified by hexose and a single 176 Da sugar (m/z 1919) shifted to m/z 2003 after esterification, consistent with the presence of six carboxyl groups. The 176 Da residue is, therefore, likely to be a hexuronic acid. Similarly, the peptide modified by hexose and two 176 Da moieties (m/z 2095) was observed at m/z 2193 after esterification, indicating both 176 Da constituents to be hexuronic acids. No further mass shift was, however, noted with the tetrasaccharide, which gave a signal at m/z 2383 after esterification, i.e. 190 Da higher than m/z 2193. Hence, the 190 Da sugar does not contain a free carboxyl group. The pentasaccharide linked to Asn13 thus has the sequence hexose (Hex)-X-hexuronic acid (HexA)-HexA-Hex-peptide, where X is a 190 Da moiety, likely to be either dimethylated hexose or the methyl ester of hexuronic acid. Experiments are currently underway to determine the nature of X and to define other structural details, including the mode of linkage and stereochemistry of each sugar residue. It is, however, already clear from the MS data presented here that the Asn13-bound glycan is very different from the oligomer of β -1-4-linked glucose subunits previously reported as linked to this residue.²⁷

Repeatedly, less of the trisaccharide-bearing species was detected, relative to the disaccharide-containing peptide. Similarly, more tetrasaccharide-modified peptide than trisaccharide-bearing species was consistently detected. These observations suggest that addition of hexuronic acid occurs relatively slowly, yet once these two subunits have been added to the growing polysaccharide, this precursor is rapidly processed to yield the tetrameric species *via* addition of the 190 Da species. Subsequent addition of the final hexose subunit also appears to be a much less efficient step than addition of the 190 Da subunit, given the relatively minor amount of the completed pentasaccharide detected, as compared to the level of tetrasaccharide.

When the N-linked glycosylation profile of the same peptide isolated from AglD-lacking cells was similarly analyzed, no pentasaccharide could be detected, although mono-, di-, tri- and tetrasaccharide species were readily observed (Figure 3(b)).

Thus, it can be concluded that AglD is involved in adding the ultimate hexose subunit to form the pentasaccharide decorating Asn13. The Asn13-containing peptide from the deletion strain, moreover, contained a greatly diminished level of the precursor tetrasaccharide glycan moiety, relative to the background strain. In addition, whereas the di- and trisaccharide-bearing species were present in the same relative ratios as in the background strain, their absolute levels were significantly reduced in the mutant strain. A similar observation was made by Chaban *et al.*²³ upon deletion of *aglA*, a gene involved in *M. voltae* flagellin N-glycosylation, with lower levels of a partially N-glycosylated tryptic peptide being isolated from the mutant cell, relative to what was obtained from the wild-type cell.

To determine whether the same pentasaccharide is found at other putative S-layer glycoprotein N-glycosylation sites and assess how the absence of *aglD* affected the glycan pattern, a second peptide including Asn83 (⁶⁵NQPLGTYDVGSGSATTPNV-TLLAPR⁹⁰) was isolated following digestion with trypsin and Glu-C. Subsequent MS analysis confirmed the peptide to be modified by a mixture of mono- (m/z 2806), di- (m/z 2982), tri- (m/z 3158), tetra- (m/z 3348) and pentasaccharide (m/z 3510) glycans of the same composition as found at Asn13 (Figure 3(c)). The Asn83-linked glycan was also affected by the absence of AglD exactly as was the pentasaccharide bound to Asn13 in the deletion cells (data not shown). By contrast, a peptide containing Asn370, also generated by joint tryptic and Glu-C treatment, was not glycosylated in either the background or the mutant cells (data not shown).

No N-glycosylation of the *H. volcanii* S-layer glycoprotein occurs upon *aglB* deletion

In addition to AglD and other predicted glycosyltransferases putatively involved in *H. volcanii* N-glycosylation, earlier efforts²⁴ had identified the *H. volcanii* homologue of Stt3, the central component of the eukaryal OST complex^{8,9} and the only OST component thus far detected in Archaea.^{1,23,24} *H. volcanii* Stt3 was implicated in S-layer glycoprotein glycosylation based on the enhanced SDS-PAGE migration of the reporter in cells deleted of the *stt3* gene.²⁴ To confirm the involvement of Stt3, now renamed AglB according to the nomenclature of Chaban *et al.*,²³ in S-layer glycoprotein N-glycosylation, MS was performed as described above. As reflected in Figure 3(d), the absence of AglB completely eliminated glycan modification at the Asn13 position, with only the peptide being detected at m/z 1581. The same held true for the Asn83-containing peptide (data not shown). These results thus confirm that *H. volcanii* AglB is responsible for OST activity in this species.

Incomplete N-glycosylation interferes with proper *H. volcanii* S-layer assembly

To assess the importance of N-glycosylation in the proper assembly of the S-layer surrounding the

H. volcanii cell (apparently composed solely of the S-layer glycoprotein²⁶), protease sensitivity of the S-layer glycoprotein was compared in the background and the *aglB* and *aglD* deletion strains. Trypsinolysis of the cells (up to 3 h) revealed the S-layer glycoprotein in the *AglD*-lacking strain to be more resistant to proteolysis than was its counterpart in the background strain (Figure 4(a)), suggesting that the aberrant glycosylation of the S-layer glycoprotein in the *AglD*-lacking strain affected the proper assembly of the S-layer. By contrast, no difference in protease susceptibility of the S-layer glycoprotein in the background and *AglB*-lacking strains was observed (Figure 4(b)).

Earlier examination of negatively stained *H. volcanii* envelope preparations revealed the S-layer as a crystalline-like lattice of hexameric complexes, each comprising six S-layer glycoproteins organized around an inwardly oriented, funnel-shaped pore³¹. Three-dimensional reconstruction of the *H. volcanii* S-layer, as well as earlier electron microscopy (EM) evidence,³² suggested this cell wall structure to

extend some 12.5 nm from the plasma membrane, implying the presence of a pseudo-periplasmic space. Moreover, it was implied that the glycan moieties of the S-layer glycoprotein provide physical support for this architecture. Thus, to more directly examine whether differential N-glycosylation of the S-layer glycoprotein in the various strains led to differences in S-layer architecture, cell envelope preparations from background, *aglB* and *aglD*-deleted strains were prepared for EM analysis using rapid freezing techniques. When isolated envelope preparations from the background WR536 strain were considered, both the plasma membrane and S-layer were readily detected (Figure 4(c), left panel). Examination of the space between these two boundaries as well as the edge of the S-layer revealed a lattice network. Cell envelopes obtained from *AglB*-lacking cells presented a similar picture (Figure 4(c), right panel). When, however, envelope preparations from *H. volcanii* cells deleted of *aglD* were similarly examined, no such symmetry was detected (Figure 4(c), middle panel).

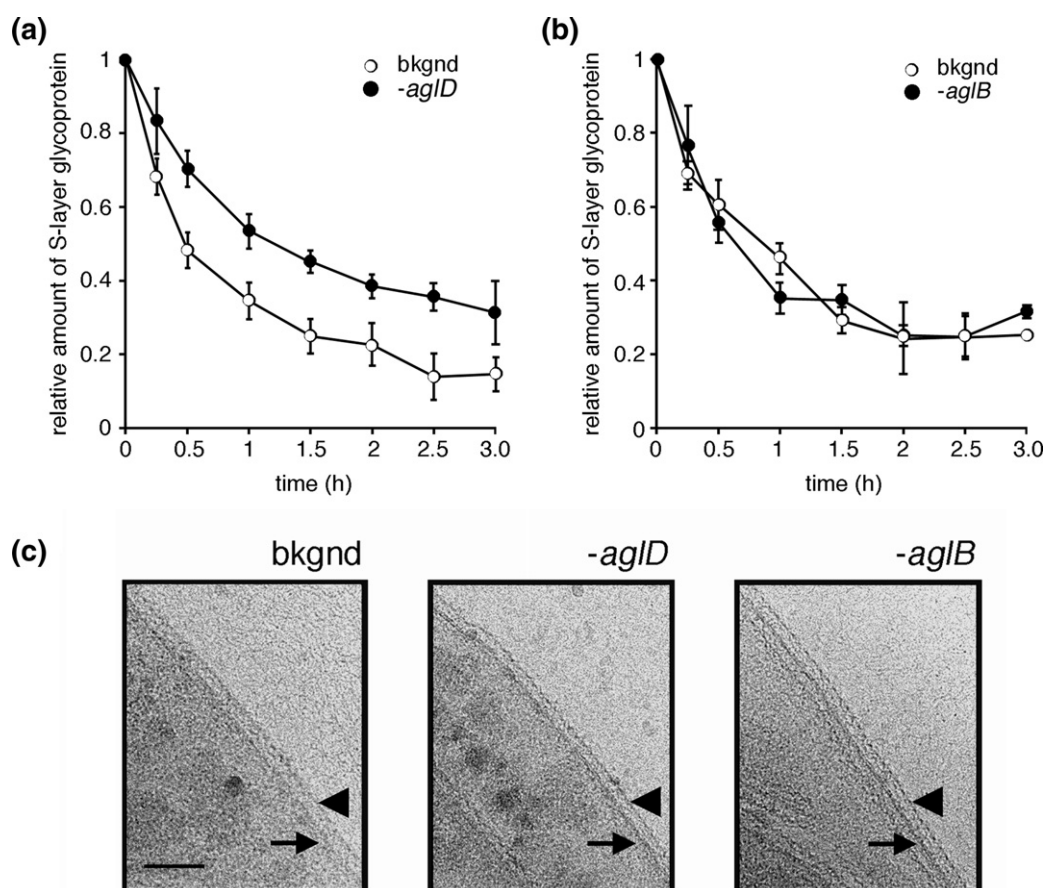


Figure 4. Perturbed S-layer glycoprotein N-glycosylation affects *H. volcanii* S-layer architecture. (a) Background strain WR536 cells (open circles) or *AglD*-lacking cells of the same strain (filled circles) were challenged with 1 mg/ml of trypsin at 37 °C. Aliquots were removed immediately prior to incubation with trypsin and at subsequent 15–30 min intervals after addition of the protease and examined by SDS–7.5% PAGE. The amount of S-layer glycoprotein remaining with time, relative to that amount found immediately prior to proteolysis, was quantified densitometrically. Each point represents the average of three experiments \pm SEM. Background cells, open circles; *AglD*-lacking cells, filled circles. (b) As in (a), only *AglB*-lacking cells were examined instead of *AglD*-lacking cells. (c) Electron micrographs of cells envelopes. Left panel, *H. volcanii* WR536 cells (bkgnd); middle panel, the same cells lacking *AglD* (*-aglD*); right panel, the same cells lacking *AglB* (*-aglB*). In each panel, the arrow points to the plasma membrane while the arrowhead points to the outer edge of the surface layer. The bar in the left panel represents 100 nm.

To determine whether the differential N-glycosylation of the S-layer glycoprotein in the various *H. volcanii* strains reflected differences in S-layer stability, the extent of S-layer glycoprotein release into the growth medium of each cell type was compared. As reflected in Figure 5(a), less S-layer glycoprotein was released from AglD-lacking cells, relative to that amount released from the background strain after 10 h. By contrast, significantly more S-layer glycoprotein was released by cells lacking AglB within the same period. These relation-

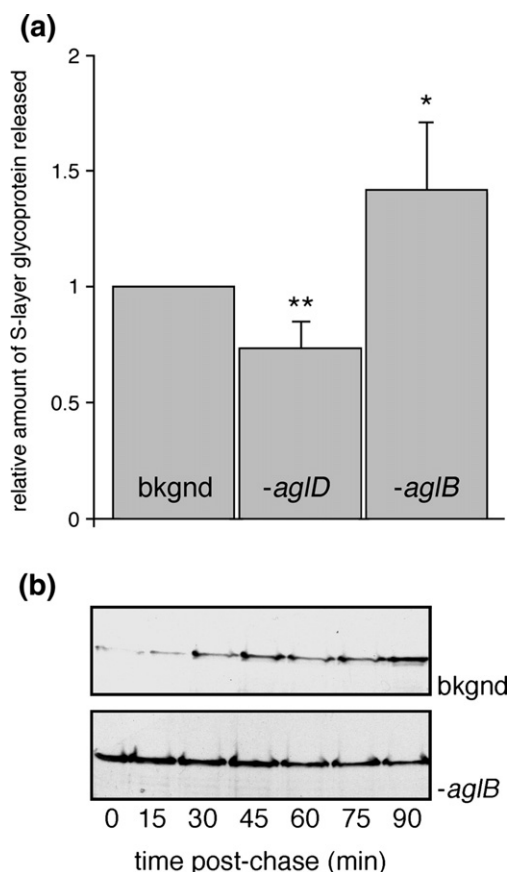


Figure 5. The S-layer glycoprotein is more readily released from *H. volcanii* cells lacking N-glycosylation capability. (a) The levels of S-layer glycoprotein released into the growth media from *H. volcanii* WR536 cells (bkgnd) or the same cells lacking either AglB (-aglB) or AglD (-aglD) after 10 h of growth were quantified densitometrically following trichloroacetic acid precipitation, SDS-PAGE and Coomassie staining. The amount of S-layer glycoprotein released from the background strain was set at a value of 1. Each bar represents the average of five separate growths for each cell type. Error bars correspond to standard deviation. The asterisk corresponds to a value being statistically significant to $p < 0.01$, while the double asterisk corresponds to a statistical significance of $p < 0.001$, as determined by student's t test. (b) Background *H. volcanii* cells or the same cells lacking AglB were pulse radiolabeled with [35 S]Cys/Met for 5 min and chased with excess Cys/Met. The growth medium of each culture was removed, the protein content precipitated, separated by SDS-7.5% PAGE and visualized by fluorography. Upper panel, background (bkgnd) cells; lower panel, AglB-lacking (-aglB) cells. Shown is a representative of four repeats.

ships also held true when the amounts of S-layer glycoprotein released from each cell type were compared after 18 h of growth (data not shown).

To further consider whether incomplete or absent N-glycosylation affected S-layer turnover, metabolic pulse-chase radiolabeling was performed. Background cells as well as the same cells deleted of *aglB* or *aglD* were grown to the same optical density in minimal medium and pulse radiolabeled with 14 μ Ci of [35 S]Cys/Met for 5 min, after which time excess cold Cys/Met was added. Equivalent aliquots were collected every 15 min and the growth medium was isolated for analysis by SDS-PAGE and fluorography. Over the first 15–30 min of chase, radiolabeled S-layer glycoprotein began to accumulate in the medium of the background strain (Figure 5(b), upper panel). Over the next hour, a relatively consistent level of S-layer glycoprotein was detected. A comparable picture was obtained when cells deleted of *aglD* were similarly considered (data not shown). By contrast, radiolabeled S-layer glycoprotein was detected in the medium of cells lacking AglB from the onset of the chase period at higher levels than detected in the background strain medium, with the amount of released 35 S incorporating S-layer glycoprotein starting to decrease some 45 min following the onset of the chase (Figure 5(b), lower panel). Finally, analysis of the cellular fraction of the different cell types confirmed that comparable amounts of radioactivity had been incorporated into the S-layer glycoprotein and other proteins during the pulse phase of the experiment (results not shown).

Together, these studies indicate that partial processing of S-layer glycoprotein N-glycosylation sites compromises the proper assembly of the protein shell surrounding *H. volcanii* cells. Moreover, while N-glycosylation is not, *per se*, essential for proper S-layer assembly, the absence of this post-translational modification affects S-layer stability.

Growth in high salt is hindered by the absence or perturbation of S-layer glycoprotein N-glycosylation

To determine whether the complete or partial absence of N-glycosylation affected the ability of *H. volcanii* to grow across a range of salt concentrations, cells of the background strain, as well as cells of the same strain deleted of either *aglB* or *aglD*, were grown in rich medium containing 1.75, 3.5 or 4.8 M NaCl. As reflected in Figure 6, the background strain grew at all three salt concentrations, although the rate of growth decreased as the salt level increased. In the case of AglD-lacking cells (Figure 6(a)), growth was slightly slower than the background strain in the presence of 1.75 or 3.5 M NaCl, as reported.²⁴ Growth of the deletion strain was significantly perturbed relative to the background species in the presence of 4.8 M NaCl. A similar picture was obtained when AglB-lacking cells were grown in rich medium containing a range of NaCl concentrations (Figure 6(b)). The deletion strain grew at essentially the same rate as background cells in the presence of

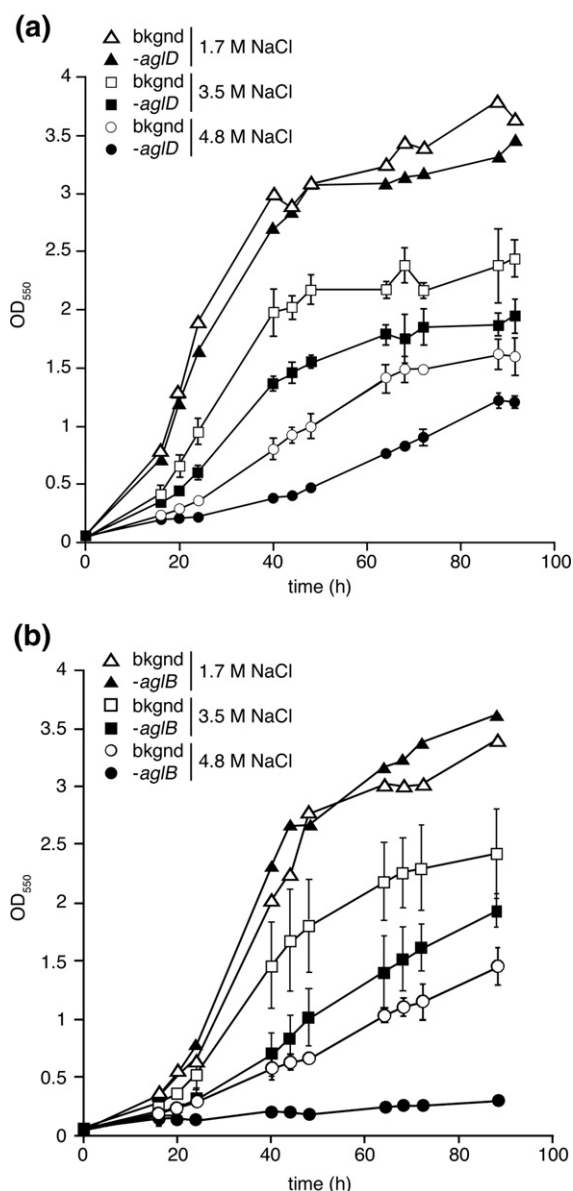


Figure 6. *H. volcanii* cells lacking AglB or AglD grow slower than the background strain at elevated NaCl concentrations. Background strain WR536 cells (open symbols) or AglB or AglD-lacking cells of the same strain (filled symbols) were grown in rich medium containing 1.75 M NaCl (triangles), 3.5 M NaCl (squares) or 4.8 M NaCl (circles). Growth was measured spectrophotometrically at an optical density of 550 nm. (a) Growth curves of background (bkgnd) and AglD-lacking (-aglD) cells. (b) Growth curves of background (bkgnd) and AglB-lacking (-aglB) cells. The growth curves of cells grown in medium containing 1.75 M NaCl represent the results of a single growth, while the growth curves of cells grown in medium containing 3.5 or 4.8 M NaCl represent the results of two to three growths \pm standard deviation.

1.75 M NaCl, and, again in agreement with earlier studies²⁴ slightly slower than the background strain in medium containing 3.5 M NaCl. When the mutant strain was grown in 4.8 M NaCl, growth was considerably slower than what was observed for background cells. By contrast, when cells deleted of

dpm1-B, a gene previously implicated in *H. volcanii* N-glycosylation,²⁴ were similarly challenged, no decrease in growth rate was observed upon elevation of salt concentrations (data not shown).

Discussion

Description of the N-glycosylated nature of the *H. salinarum* S-layer glycoprotein some 30 years ago represented the first challenge to the dogma that only eukaryotes were capable of performing such post-translational modification. Since, it has become clear that like Archaea, Bacteria are also capable of performing N-glycosylation. While substantial progress has been made in understanding bacterial N-glycosylation,³ little is known of the steps involved in the parallel process in Archaea. Of late, however, initial steps have been taken towards remedying this situation.^{23,24,33}

In continuing our delineation of the *H. volcanii* N-glycosylation process, MS was employed to provide insight into the composition of the glycan moiety decorating the Asn13 and Asn83 positions of the S-layer glycoprotein, a well-characterized reporter of this post-translational modification^{26,27,30} in cells deleted of genes previously implicated in the process. Of the seven putative sequons found within the S-layer glycoprotein, four had been previously reported to be modified in the native protein; Asn13 and Asn505 were portrayed as bearing linear chains of β -1-4-linked glucose residues, Asn274 was described as being modified by a glucose and idose-containing moiety, while Asn279 was said to carry a polysaccharide containing glucose, idose and galactose.^{26,27} In addition, total sugar analysis of the S-layer glycoprotein also reported the presence of mannose.²⁷ Later examination of the dolichol-linked oligosaccharide content of *H. volcanii* cells, presumably involved in the N-glycosylation process, revealed the presence of phosphodolichol-linked mannosyl galactose, sulfated or phosphorylated dihexose as well as a sulfated or phosphorylated tetrasaccharide, shown by GC/MS to include mannose, galactose and rhamnose in a 2:1:1 ratio.³⁴ The glycan profile of the *H. volcanii* S-layer glycoprotein is further complicated by the fact that the protein experiences not only N-glycosylation but also O-glycosylation at a cluster of Thr residues located near the C terminus of the protein.²⁶ Here, however, we find the glycan moiety linked to Asn13 and Asn83 of the native *H. volcanii* S-layer glycoprotein corresponds to a pentasaccharide containing two hexoses, two hexuronic acids and a 190 *m/z* subunit, possibly corresponding to a methylated hexuronic acid or a di-methylated hexose. Several possible explanations can be offered for the discrepancies between the present findings and previous studies. Detection of multiple β -1-4 linked glucose residues²⁷ can commonly result from contaminating cellulose-like polysaccharides within a sample. Moreover, were the reported phosphodolichol-linked glycan content of *H. volcanii*³⁴ reflecting only a partial census of lipid-bound poly-

saccharides in this species, then the absence of the pentasaccharide detected here linked to phosphodolichol would be explained. Indeed, the previously defined lipid-linked glycan structures may be preferentially involved in the biosynthesis of glycolipids^{35,28} or other *H. volcanii* glycoproteins.^{28,30}

Having defined N-linked glycans decorating the *H. volcanii* S-layer glycoprotein, the actions of two enzymes involved in N-glycosylation process, i.e. *aglB* and *aglD*, were characterized. *AgID* is involved in catalyzing the addition of the final hexose to the pentasaccharide decorating at least two sequon Asn residues, namely Asn13 and Asn83. In terms of its topology, *AgID* includes a soluble, cytoplasm-facing N-terminal half, associated with the membrane *via* the integral C-terminal portion of the molecule. Predicted to span the membrane six times, *AgID* presents a topology reminiscent of those eukaryal glycosyltransferases containing active sites facing the ER lumen, responsible for the transfer of mannose or glucose residues from charged dolichol carriers to the pyrophosphodolichol-bound heptasaccharide following its reorientation from the cytoplasmic to the luminal face of the ER membrane. By contrast, those glycosyltransferases presenting domains homologous to the soluble N-terminal portion of *AgID* correspond to single membrane-spanning enzymes that employ soluble nucleotide-activated monosaccharides in assembling the heptasaccharide found on the cytoplasm-facing ER membrane-embedded dolichol pyrophosphate carrier.^{1,7} Further experimentation is, therefore, required before it can be concluded whether the oligosaccharides decorating the *H. volcanii* S-layer glycoprotein are assembled from activated soluble sugars or from lipid-linked subunits, thus defining the actual role played by *AgID* in this processing event.

AgIB, as the sole component of the OST detected in *H. volcanii*,²⁴ is responsible for transferring a pentasaccharide moiety, again presumably from a dolichol phosphate carrier,³⁴ to at least two S-layer glycoprotein sites, namely Asn13 and Asn83. The observation that *H. volcanii* *AgIB* can transfer truncated glycan structures to the S-layer glycoprotein, as in *aglD*-deleted cells, suggests a relaxed substrate specificity of the enzyme, as reported for eukaryal OSTs,^{36,37} *C. jejuni* *PglB*^{12,13} and *AgIB* from the methanoeocyte *M. voltae*.²³ However, unlike *PglB*,¹³ *H. volcanii* *AgIB* is capable of transferring not only fully assembled oligosaccharides, but also precursor glycans. Indeed, while differences in the relative amounts of the precursor oligosaccharide-bearing glycopeptides could reflect the differential kinetics of the glycosyltransferases involved in glycan assembly, such quantitative differences could also reflect differential processing by *AgIB* (or the putative enzyme responsible for transferring dolichol-linked oligosaccharides across the archaeal plasma membrane) of these precursors. *H. volcanii* *AgIB* is, moreover, unusual in that it appears to transfer polysaccharides from phospho- rather than pyrophosphodolichol carriers.³⁴

The absence of *aglD* resulted in the generation of an S-layer displaying altered protease sensitivity and an

increased degree of disorder. Deletion of *H. volcanii* *aglB*, and hence prevention of S-layer glycoprotein N-glycosylation, led to enhanced release of the protein into the growth medium. Taken together, the results imply that not only is complete N-glycosylation important for realizing correct *H. volcanii* S-layer architecture but that stable association of the S-layer glycoprotein within the S-layer requires such modification. Accordingly, both aberrant and absent N-glycosylation compromised the ability of *H. volcanii* to grow at high salt concentrations. Thus, N-glycosylation can be considered a post-translational modification designed to allow *H. volcanii* to remain intact in the face of the hypersaline environment in which these cells exist. It should be noted, however, that the S-layer glycoprotein experiences both N and O-glycosylation.²⁶ As such, the effects on the S-layer glycoprotein, the S-layer and the intact cell observed upon either modulation or loss of N-glycosylation may present only a partial picture of the importance of S-layer glycoprotein glycosylation to *H. volcanii* cells.

The observation that not all S-layer glycoprotein sequons are modified (e.g. Asn370) raises the question of how such sites differ from sequons that include modified Asn residues, such as Asn13 and Asn83. Unfortunately, the limited dataset considered here does not allow for detailed assessment of the regions surrounding modified and unmodified *H. volcanii* S-layer glycoprotein sequons. Indeed, recent analysis of the amino acid composition of those archaeal sequons experimentally verified as being modified as well as the composition of the 20 up- and downstream residues failed to reveal any consistent sequence traits, apart from a requirement for the Asn-X-Ser/Thr motif, where X is any residue apart from Pro.³³ As such, deciphering the rules governing whether a given archaeal sequon is modified will have to wait for more experimental data to allow for development of appropriate predictive algorithms.

With the identification of gene products directly involved in *H. volcanii* N-glycosylation and in *M. voltae*,²³ a map of steps involved in this post-translational modification in Archaea and, therefore, across evolution, is beginning to emerge. Continued efforts will not only serve to fill the numerous gaps in our understanding of archaeal N-glycosylation but will also offer insight into possible links between this protein processing event and the ability of archaeal polypeptides to remain folded and functional in the face of conditions that would normally lead to protein denaturation, loss of solubility and aggregation, conditions eventually resulting in cell death.

Materials and Methods

Data base accession code

The nucleotide sequence of *H. volcanii* *AgID* has been deposited in the EMBL nucleotide sequence database (accession number AM698042).

Growth conditions

The *H. volcanii* background strain WR536 and the same strain deleted for either *alg5-A/aglD* or *stt3/aglB*²⁴ were grown in complete medium containing 3.4 M NaCl, 0.15 M MgSO₄·7H₂O, 1 mM MnCl₂, 4 mM KCl, 3 mM CaCl₂, 0.3% (w/v) yeast extract, 0.5% (w/v) Tryptone, 50 mM Tris-HCl (pH 7.2) at 40 °C.³⁸

Metabolic labeling with [¹⁴C]glucose, -galactose or -mannose

To perform metabolic labeling with [¹⁴C]glucose, -galactose or -mannose, *H. volcanii* strain WR536 background, *aglB* and *aglD*-depleted cells were grown in minimal medium.³⁹ When the cultures reached an A₅₅₀ of 0.5, the cultures were supplemented with 12 μCi of [¹⁴C]glucose, -galactose or -mannose per ml cell culture and grown at 40 °C for an additional 40 min. The protein contents of the radiolabeled cells were separated by SDS-PAGE and examined by Coomassie staining and fluorography. [¹⁴C]Glucose (230–270 mCi/mmol), [¹⁴C]galactose (>200 mCi/mmol) and [¹⁴C]mannose (200–310 mCi/mmol) were obtained from Amersham (Buckingham, UK). Densitometry was performed using IPLab Gel software (Signal Analytics, Vienna VA).

Pulse-chase radiolabeling

H. volcanii strain WR536, *aglB*- and *aglD*-depleted cells were grown in minimal medium³⁹ to A₅₅₀=0.5. [³⁵S]Cys/Met (14.3 μCi/ml) was added for 5 min, after which time unlabeled Cys/Met was added to a final concentration of 1 mM. Aliquots were removed immediately prior to and at 15 min intervals following addition of the unlabeled Cys/Met and centrifuged (8000g, 10 min, room temperature). The supernatant, corresponding to the medium, was removed and its protein content was precipitated with 15% (w/v) trichloroacetic acid. The resulting pellet was washed in ice-cold acetone and boiled in SDS-PAGE sample buffer. Following electrophoresis, the S-layer glycoprotein was visualized by fluorography using Kodak X-Omat film. The Redivue ³⁵S radiolabeling mixture (>1000 Ci/mmol) came from Amersham (Buckingham, UK).

Concanavalin A overlay

ConA overlay blotting of the protein content of *H. volcanii* WR536 cells and the same strain deleted for *aglD* or *alg5-B*²⁴ was performed following protein separation by SDS-PAGE and transfer to a nitrocellulose membrane (0.45 μm; Scheicher and Schuell, Dassel, Germany). The membrane was incubated with 10 μg/ml of horseradish peroxidase (HRP)-conjugated ConA (Sigma, St. Louis MO) in PBS containing 1 mM CaCl₂, 1 mM MnCl₂, 0.5% (v/v) Tween 20 and 5% (w/v) low-fat milk powder for 1 h. For visualization of ConA-labeled proteins, the membrane was developed using the ECL enhanced chemiluminescence kit (Amersham Pharmacia Biotech, Piscataway, NJ).

Mass spectrometry

For in-gel tryptic digestion of the *H. volcanii* S-layer glycoprotein from cells of the background strain, or the

same strain depleted of *aglB* or *aglD*, samples were run on 10% pre-cast gels (Invitrogen, Paisley, UK) and stained with Novex Colloidal blue stain (Invitrogen). Relevant bands were excised, destained in 400 μl of 50% (v/v) acetonitrile in 0.1 M ammonium bicarbonate (pH 8.4) and dried using a SpeedVac drying apparatus. The gel slices were rehydrated in 20 μl of trypsin working solution (Promega sequencing grade modified trypsin, prepared according to manufacturer's instructions) and incubated overnight at 37 °C. The supernatant was removed and the tryptic digest was halted by addition of 50 μl of 0.1% (v/v) trifluoroacetic acid for 10 min at 37 °C. The supernatant was removed and the peptides were further extracted with 200 μl of 60% (v/v) acetonitrile/0.1% trifluoroacetic acid for 15 min at 37 °C. The supernatant was removed and pooled with the previous supernatant. Both extraction steps were repeated and the supernatants pooled. The volume of the combined supernatants was subsequently reduced using a SpeedVac drying apparatus. For double digest with Glu-C, aliquots of the tryptically digested samples were dried using a SpeedVac, then re-suspended in 20 μl of Glu-C working solution (Roche sequencing grade endoproteinase Glu-C, prepared according to manufacturer's instructions). MALDI TOF MS was performed using a PerSeptive Biosystems Voyager DE STR mass spectrometer (Applied Biosystems, Foster City, CA) in the reflectron mode and set for delayed extraction. Samples were analyzed using the matrix α-cyano-4-hydroxy-cinnamic acid (Aldrich). Sequazyme peptide mass standards were used as external calibrants (Applied Biosystems).

For offline liquid chromatography MALDI TOF/TOF-MS analysis, tryptic peptides were separated using the Ultimate 3000 LC system (Dionex, Sunnyvale CA), fitted with a Pepmap analytical C-18 nanocapillary (75 μm internal diameter ×15 cm length; Dionex). The digest was loaded onto the column and eluted using solvent A (0.1% (v/v) formic acid in 2% acetonitrile and solvent B (0.1% formic acid in 90% acetonitrile), in the following gradient: 0–60% solvent B (0–36 min), 60–90% solvent B (36–37 min), 90% solvent B (37–40 min) and 100% solvent A (40–41 min). Eluting fractions were mixed with a cyano-hydroxy cinnamic acid matrix and spotted onto α metal MALDI target plate. MALDI TOF/TOF MS was performed using an Applied Biosystems 4800 mass spectrometer in the positive reflectron mode and set for delayed extraction. MS/MS was performed with the CID setting turned on. Sequazyme peptide mass standards were used as external calibrants.

Cryo-electron microscopy (EM)

Cell envelopes were prepared from *H. volcanii* strain WR536 background, *aglB* and *aglD*-depleted cells as described.³¹ For cryo-EM, a 5 μl drop of cell envelopes was applied onto glow-discharged 200 mesh carbon-coated copper grids (Quantifoil, Jena, Germany) and vitrified⁴⁰ immediately after home-made 15 nm colloidal gold was added. Data were collected using a 300 kV FEI Polara transmission EM equipped with a field-emission gun, and a Gatan post-column GIF 2002 energy filter. The cell envelopes were imaged at 4400× magnification, yielding a 4 Å pixel size at the specimen level. The micrographs were aligned to a common origin using the fiducial gold markers. To minimize systematic alignment errors, those gold markers in closest vicinity to a membrane were kept fixed in a least-squares fit, as implemented by the TOM package.⁴¹

Acknowledgements

J.E. is supported by the US Air Force Office for Scientific Research (grant FA9550-07-10057). M.A.-Q. is the recipient of a fellowship from the Israel Ministry for Foreign Affairs; O.M. is supported by the Israel Science Foundation (grant 794/06) and A.D. and H.R.M. are supported by the Biotechnology and Biological Sciences Research Council and Wellcome Trust. A.D. is a Biotechnology and Biological Sciences Research Council Professorial Fellow.

References

- Burda, P. & Aebi, M. (1999). The dolichol pathway of N-linked glycosylation. *Biochim. Biophys. Acta*, **1426**, 239–257.
- Eichler, J. & Adams, M. W. W. (2005). Post-translational protein modification in Archaea. *Microbiol. Mol. Biol. Rev.* **69**, 393–425.
- Szymanski, C. M. & Wren, B. W. (2005). Protein glycosylation in bacterial mucosal pathogens. *Nature Rev. Microbiol.* **3**, 225–237.
- Weerapana, E. & Imperiali, B. (2006). Asparagine-linked protein glycosylation: from eukaryotic to prokaryotic systems. *Glycobiology*, **16**, 91R–101R.
- Kornfeld, R. & Kornfeld, S. (1985). Assembly of asparagine-linked oligosaccharides. *Annu. Rev. Biochem.* **54**, 631–664.
- Spiro, R. G. (2002). Protein glycosylation: nature, distribution, enzymatic formation, and disease implications of glycopeptide bonds. *Glycobiology*, **12**, 43R–56R.
- Helenius, A. & Aebi, M. (2004). Roles of N-linked glycans in the endoplasmic reticulum. *Annu. Rev. Biochem.* **73**, 1019–1049.
- Kelleher, D. J. & Gilmore, R. (2006). An evolving view of the eukaryotic oligosaccharyltransferase. *Glycobiology*, **16**, 47R–62R.
- Yan, A. & Lennarz, W. J. (2005). Unraveling the mechanism of protein N-glycosylation. *J. Biol. Chem.* **280**, 3121–3124.
- Szymanski, C. M., Yao, R., Ewing, C. P., Trust, T. J. & Guerry, P. (1999). Evidence for a system of general protein glycosylation in *Campylobacter jejuni*. *Mol. Microbiol.* **32**, 1022–1030.
- Linton, D., Allan, E., Karlyshev, A. V., Cronshaw, A. D. & Wren, B. W. (2002). Identification of N-acetylgalactosamine-containing glycoproteins PEB3 and CgpA in *Campylobacter jejuni*. *Mol. Microbiol.* **43**, 497–508.
- Glover, K. J., Weerapana, E., Numao, S. & Imperiali, B. (2005). Chemoenzymatic synthesis of glycopeptides with PglB, a bacterial oligosaccharyl transferase from *Campylobacter jejuni*. *Chem. Biol.* **12**, 1311–1315.
- Linton, D., Dorell, N., Hitchen, P. G., Amber, S., Karlyshev, A. V., Morris, H. R. *et al.* (2005). Functional analysis of the *Campylobacter jejuni* N-linked protein glycosylation pathway. *Mol. Microbiol.* **55**, 1695–1703.
- Wacker, M., Linton, D., Hitchen, P. G., Nita-Lazar, M., Haslam, S. M., North, S. J. *et al.* (2002). N-linked glycosylation in *Campylobacter jejuni* and its functional transfer into *E. coli*. *Science*, **298**, 1790–1793.
- Kelly, J., Jarrell, H., Millar, L., Tessier, L., Fiori, L. M., Lau, P. C. *et al.* (2006). Biosynthesis of the N-linked glycan in *Campylobacter jejuni* and addition onto protein through block transfer. *J. Bacteriol.* **188**, 2427–2434.
- Szymanski, C. M., Burr, D. H. & Guerry, P. (2002). *Campylobacter* protein glycosylation affects host cell interactions. *Infect. Immun.* **70**, 2242–2244.
- Hendrixson, D. R. & DiRita, V. J. (2004). Identification of *Campylobacter jejuni* genes involved in commensal colonization of the chick gastrointestinal tract. *Mol. Microbiol.* **52**, 471–484.
- Karlyshev, A. V., Everest, P., Linton, D., Cawthraw, S., Nevell, D. G. & Wren, B. W. (2004). The *Campylobacter jejuni* general glycosylation system is important for attachment to human epithelial cells and in the colonization of chicks. *Microbiology*, **150**, 1957–1964.
- Mescher, M. F. & Strominger, J. L. (1976). Purification and characterization of a prokaryotic glycoprotein from the cell envelope of *Halobacterium salinarum*. *J. Biol. Chem.* **251**, 2005–2014.
- Lechner, J. & Sumper, M. (1987). The primary structure of a prokaryotic glycoprotein. Cloning and sequencing of the cell surface glycoprotein gene of halobacteria. *J. Biol. Chem.* **262**, 9724–9729.
- Schaffer, C., Graninger, M. & Messner, P. (2001). Prokaryotic glycosylation. *Proteomics*, **1**, 248–261.
- Upreti, R. K., Kumar, M. & Shankar, V. (2003). Bacterial glycoproteins: functions, biosynthesis and applications. *Proteomics*, **3**, 363–379.
- Chaban, B., Voisin, S., Kelly, J., Logan, S. M. & Jarrell, K. F. (2006). Identification of genes involved in the biosynthesis and attachment of *Methanococcus voltae* N-linked glycans: insight into N-linked glycosylation pathways in Archaea. *Mol. Microbiol.* **61**, 259–268.
- Abu-Qarn, M. & Eichler, J. (2006). Protein N-glycosylation in Archaea: defining *Haloferax volcanii* genes involved in S-layer glycoprotein glycosylation. *Mol. Microbiol.* **61**, 511–525.
- Marchler-Bauer, A., Anderson, J. B., Cherukuri, P. F., DeWeese-Scott, C., Geer, L. Y., Gwadz, M. *et al.* (2005). CDD: a conserved domain database for protein classification. *Nucl. Acids Res.* **33**, D192–D166.
- Sumper, M., Berg, E., Mengele, R. & Strobel, I. (1990). Primary structure and glycosylation of the S-layer protein of *Haloferax volcanii*. *J. Bacteriol.* **172**, 7111–7118.
- Mengele, R. & Sumper, R. (1992). Drastic differences in glycosylation of related S-layer glycoproteins from moderate and extreme halophiles. *J. Biol. Chem.* **267**, 8182–8185.
- Zhu, B. C., Drake, R. R., Schweingruber, H. & Laine, R. A. (1995). Inhibition of glycosylation by amphomycin and sugar nucleotide analogs PP36 and PP55 indicates that *Haloferax volcanii* beta-glycosylates both glycoproteins and glycolipids through lipid-linked sugar intermediates: evidence for three novel glycoproteins and a novel sulfated dihexosyl-archaeol glycolipid. *Arch. Biochem. Biophys.* **319**, 355–364.
- Eichler, J. (2000). Novel glycoproteins of the halophilic archaeon *Haloferax volcanii*. *Arch. Microbiol.* **173**, 445–448.
- Eichler, J. (2001). Post-translational modification of the S-layer glycoprotein occurs following translocation across the plasma membrane of the haloarchaeon *Haloferax volcanii*. *Eur. J. Biochem.* **268**, 4366–4373.
- Kessel, M., Wildhaber, I., Cohen, S. & Baumeister, W. (1988). Three-dimensional structure of the regular surface glycoprotein layer of *Halobacterium volcanii* from the Dead Sea. *EMBO J.* **7**, 1549–1554.
- Blaurock, A. E., Stoeckenius, W., Oesterhelt, D. & Scherfhof, G. L. (1976). Structure of the cell envelope of *Halobacterium halobium*. *J. Cell. Biol.* **71**, 1–22.
- Abu-Qarn, M. & Eichler, J. (2007). An analysis of amino acid sequences surrounding archaeal glycoprotein sequons. *Archaea*, **2**, 73–81.

34. Kuntz, C., Sonnenbichler, J., Sonnenbichler, I., Sumper, M. & Zeitler, R. (1997). Isolation and characterization of dolichol-linked oligosaccharides from *Haloferax volcanii*. *Glycobiology*, **7**, 897–904.
35. Torreblanca, M., Rodriguez-Valera, F., Juez, G., Ventosa, A., Kamekura, M. & Kates, M. (1986). Classification of non-alkaliphilic halobacteria based on numerical taxonomy and polar lipid composition, and description of *Haloarcula* gen. nov. and *Haloferax* gen. nov. *Syst. Appl. Microbiol.* **8**, 89–99.
36. Turco, S. J., Stetson, B. & Robbins, P. W. (1977). Comparative rates of transfer of lipid-linked oligosaccharides to endogenous glycoprotein acceptors in vitro. *Proc. Natl Acad. Sci. USA*, **74**, 4411–4414.
37. Munoz, M. D., Hernandez, L. M., Basco, R., Andaluz, E. & Larriba, G. (1994). Glycosylation of yeast exoglucanase sequons in alg mutants deficient in the glucosylation steps of the lipid-linked oligosaccharide. Presence of glucotriose unit in Dol-PP-GlcNAc2-Man9Glc3 influences both glycosylation efficiency and selection of N-linked sites. *Biochim. Biophys. Acta*, **1201**, 361–366.
38. Mevarech, M. & Werczberger, R. (1985). Genetic transfer in *Halobacterium volcanii*. *J. Bacteriol.* **162**, 461–462.
39. Kauri, T., Wallace, R. & Kushner, D. J. (1990). Nutrition of the halophilic archaeobacterium, *Haloferax volcanii*. *Syst. Appl. Microbiol.* **13**, 14–18.
40. Dubochet, J., Adrian, M., Chang, J. J., Homo, J. C., Lepault, J., McDowell, A. W. & Schultz, P. (1988). Cryo-electron microscopy of vitrified specimens. *Quart. Rev. Biophys.* **21**, 129–228.
41. Nickell, S., Forster, F., Linaroudis, A., Net, W. D., Beck, F., Hegerl, R. *et al.* (2005). TOM software toolbox: acquisition and analysis for electron tomography. *J. Struct. Biol.* **149**, 227–234.